Critical scattering function in a binary fluid mixture: A study of sodium-deuteroammonia solution at the critical concentration by small-angle neutron scattering

Pierre Damay and Françoise Leclercq
Laboratoire de Chimie-Physique, Ecole des Hautes Etudes Industrielks, 13 rue de Toul, 59046 Lille CEDEX, France

Pierre Chieux
Institut Laue-Langevin, 156X, 38042 Grenoble CEDEX, France
(Received 30 January 1989)

Small-angle neutron scattering experiments have been performed on the Na-ND_3 mixture of critical composition. Neutrons are very sensitive to the fluctuations of concentration in this system (high contrast). This allowed good statistics for a reasonable counting time, typically 0.5% at each value of the momentum transfer q for a 40-min run. Momentum transfers q between 0.008 and 0.067 Å^{-1} were investigated with the chosen experimental setup. Using several approximations of the scattering function at small $x=q\xi$, and after very careful data correction, the correlation length ξ has been determined with a good precision (2% for $\xi<300$ Å). The experimental scaling function $g(q\xi)$ was then fitted in the whole x range using different approximate equations discussed in literature. A value of the critical index $\eta=0.030\pm0.0015$ was thus found with a precision not yet obtained from experiments. A lower limit for the validity of the scaling hypothesis is given for the first time: $2-\eta-\gamma/\nu\leq0.002$. These results reconcile neutron scattering results with those obtained with light scattering and are in favor of renormalization-group-theory predictions for the three-dimensional Ising model.

I. INTRODUCTION

Much effort has been devoted to the study of the critical scattering intensity in three-dimensional (3D) systems mainly to characterize the deviations from the classical Ornstein-Zernike (OZ) equation.[1,2] Exact analytical results are available in two dimensions;[3] they clearly show the inadequacy of the OZ equation at large scattering angle, or more exactly at large value of $x=q\xi$ (where ξ is the correlation length). In three dimensions there are no analytical or exact results, but several approximations, whose accuracy depends on the x range, have been discussed in detail in literature.[1-5]

At large values of x, the shape of the critical scattering function is mainly governed by the critical index η which was first introduced by Fisher.[6] This critical index has been evaluated for the three-dimensional Ising model by high-temperature series expansion[7] ($\eta=0.041\pm0.006$) and by renormalization methods[8] ($\eta=0.031\pm0.004$). The difference found between the two methods seems irreducible.

It is very difficult to obtain a precise value of η from experiments; indeed, this index is not measured directly but only as $2-\eta$ as pointed out by Sengers.[5] From x rays or light scattering experiments, the values of η vary from 0.016 ± 0.016 to 0.030 ± 0.025. These values are in better agreement with renormalization-group-theory predictions than with high-temperature series expansion but the uncertainty is very large ($\approx100\%$). The critical regime ($x\gg1$) is reached in extreme experimental conditions with light (large values of ξ obtained only very near the critical point).

The critical regime is easily reached with neutrons, and then more precise results could reasonably be expected but the observed values of η are unexpectedly very different from theoretical predictions and from experimental results obtained with other techniques. Indeed, if one excepts the recent value given by Schwahn,[9] the values obtained by neutron scattering vary from 0.08 to 0.11 ± 0.03.[5]

The present paper reports results and an analysis of the static critical scattering function obtained by small-angle neutron scattering (SANS) for the Na-ND_3 solution at critical concentration. This system has been chosen for the very high sensitivity of neutrons to its concentration fluctuations Sec. III (contrast). Great care has been taken to optimize the sample environment, mostly to achieve the best temperature stabilization and to prevent (or detect) temperature and concentration gradients (Sec. II).

Experimental conditions are reported briefly in Sec. IV. It is found that correction for inelasticity may be neglected at least with the chosen experimental setup (Sec. V). The same result was already obtained by Schneider *et al.* in their SANS study of the isobutiric-D_2O system with similar experimental conditions.[10]

An important task in SANS is to remove noncritical scattering from the observed spectra. This has been achieved by subtracting from each run a "high-temperature" run corrected for density and for the remaining critical intensity (Sec. VI).

Several approximate equations of the scattering function and their validity range are discussed in Sec. VII.

These equations are used in least-square-fitting procedures. Detail of the calculation methods is discussed in Sec. VIII; it is shown how the errors have been handled to obtain a reliable "goodness of the fit" test. The amplitude of the concentration fluctuations $S_{cc}(0)$ and the correlation length of these fluctuation ξ are then determined using different approximations in Sec. IX. The corresponding critical indices γ and ν are calculated in Sec. X from the temperature dependence of $S_{cc}(0)$ and ξ, respectively. A first evaluation of the index η is also obtained assuming scaling hypothesis $2-\eta=\gamma/\nu$.

The shape of the critical scattering function in the intermediate and large x range is discussed in Sec. XI. In a first step, the fits are performed on each run at constant temperature; then, using scaling, all data are regrouped as a function of the single variable $x=q\xi$.

A short account of these results has already been given[11] (determination of the index η). The results obtained from scaling were then preliminary and the values reported here are slightly different. A more precise determination of the critical parameters (critical temperature, etc.) and of the correlation lengths and a thorough discussion of the approximate equations used in the fits led to the present values. These problems and the results are finally discussed in Sec. XII.

II. SAMPLE AND SAMPLE ENVIRONMENT

Pure metallic sodium has been pulled under vacuum in a 1-mm calibrated glass tubing. Sodium from a known length of this tubing is then distilled three times under high vacuum (10^{-7} torr). If the distillation is carried out very slowly in quartz cells, the final weight of metal may be predicted within a percent.

The amount of deuterated ammonia (99.75% D from the CEA, Saclay, France) is determined by gas volumetric analysis (p,V,T measurement using a first order nonideal-gas correction). The relative uncertainty on the pressure, volume, and temperature measurements are respectively 5×10^{-4}, 10^{-3}, and 3×10^{-3}, ending with an uncertainty of 4.5×10^{-3} on the ammonia weight.

From the many results found in literature, the critical sodium concentration may be evaluated between $x_{Na}=0.0412$ and 0.0416 for the protonated system. It has been shown with the lithium NH_3 and ND_3 solutions that deuteration had little effect on the critical concentration.[12] The sample used in the experiment was a mixture of $3.278\times10^{-3}\pm3\times10^{-5}$ M Na in $75.77\times10^{-3}\pm3\times10^{-4}$ M ND_3, i.e., $x_{Na}=0.04147\pm0.00062$.

The solution has been prepared in a 8-mm inside diameter quartz tubing free of protons. The length of the cell was 7 cm and the solution filled 60% of the volume; the amount of ammonia in the gas phase was then negligible in the working temperature range (less than 0.13 mM in the 200–270-K range).

A specially designed sample holder equipped with a high-performance temperature control was inserted in a standard ILL cryostate (Institut Laue Langevin in Grenoble). The temperature stabilization in the standard equipment is 0.01 deg at one point inside the cryostat chamber with a pressure less than 1 torr of helium as a gas exchange; the temperature gradient along the vertical axis is given as 0.02 deg/cm.

The insert is composed of five pieces (Fig. 1). One piece is an insulating plate which connects the insert to the standard stainless-steel top-loading cane. Another piece is an aluminum cylindric block (diameter 35 mm and 30 mm high). The block is surrounded by a 50-W insulated resistor (heater) and equipped with a calibrated platinum thermometer. The sample holder, tightly connected to the block, is a hollow aluminum cylinder (20-mm outside diameter, 10.3-mm inside diameter, and 70 mm high). Two windows are carved along the path of the neutron beam (10×40 mm^2). The holder is enfolded with a 0.5-mm pure copper shield (99.99% from Goodfellow company) which has been proven to diffuse neutrons very little at small angles. The sample is introduced from the bottom of the holder. The temperature near the sample is measured using a second platinum thermometer. Two external shieldings, hollow cylinders, made of 5-mm-thick aluminum are fixed to the block in order to reduce temperature gradients. As shown for the sample holder, both shields have been cut along the neutron beam. The inner cylinder has been covered with a 0.05-mm aluminum fold to prevent gas exchange convection. The outer shield is covered with a 0.5-mm-thick cadmium sheet. Two windows (8×10 mm^2) have been carefully cut out of the cadmium fold; they precisely defined the size of the neutron beam which is allowed to cross either the upper or the lower part of the solution. The windows are separated by 5 mm of cadmium positioned on the meniscus seen after phase separation; the distance between the two centers of diffusion is equal to 15 mm. A thick cadmium sheet fixed on the outer part of the cryostat may be moved up and down to open the lower or upper

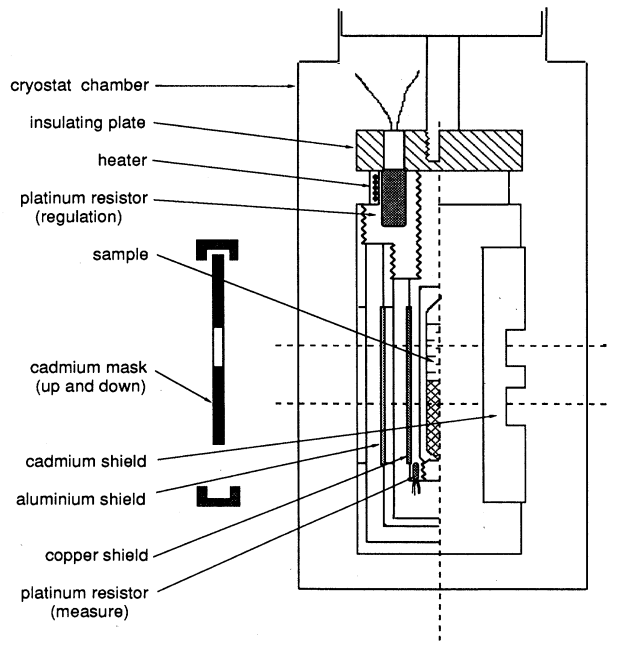

FIG. 1. Detail of the sample holder. The temperature stabilization was better than 5×10^{-4} K and the temperature gradient along the sample was less than 1.5×10^{-3} K.

window.

The main purpose of the insert was to minimize temperature gradients and to improve the temperature control; this has been achieved using a high-performance controller and an ac bridge (ASL, F16); it was then possible to stabilize the temperature of the insert with 5×10^{-4} deg. The best performance was observed for a temperature difference between the cryostat and the insert chosen between 0.1° and 0.8°, in which case temperature fluctuations were constrained within (2×10^{-4})°. The use of an ac bridge has the advantage to reduce any long-time temperature bias; the best stabilization could easily be conserved for several hours.

Careful checks of temperature gradient along the sample have been made using the difference signal read from the two thermometers. It was found that this difference was approximately a linear function of the difference $\Delta T=T_{\text{insert}}-T_{\text{cryostat}}$ for a 0°–20° interval [(1.5×10^{-3})° per degree]. Then the maximum gradient along the 4-cm height of solution has been evaluated to less than (1.5×10^{-3})° since working values of ΔT were kept below 1°. It was found that values of ΔT would better be chosen larger than 0.10° to prevent any spurious coupling between the two regulation stages.

III. CONTRAST

Following the formalism proposed by Bhatia and Thornton,[13] the coherent neutron diffusion, in the case of a binary mixture, may be written as the weighted sum of three partial structure factors:

$$\frac{1}{N}\frac{d\sigma}{d\Omega}=\langle b^2\rangle S(\mathbf{q})=\langle b\rangle^2 S_{NN}(\mathbf{q})+\langle \Delta b\rangle^2 S_{cc}(\mathbf{q}) +2\langle b\rangle\langle \Delta b\rangle S_{Nc}(\mathbf{q}) , \quad (1)$$

where $S(\mathbf{q})$ is the structure factor and $S_{\alpha\beta}(\mathbf{q})$ are partial structure factors, $\mathbf{q}$ is the momentum transfer vector $\mathbf{q}=\mathbf{k}-\mathbf{k}_0$, $\langle b\rangle=c_1b_1+c_2b_2$, and $\langle \Delta b\rangle=b_1-b_2$; c_1, c_2, b_1, and b_2 are the concentrations and scattering lengths of the two constituents ($c_1+c_2=1$), and N is the total number of atoms (it may be the number of molecules when the scattering is observed at small angle).

Near the critical point the total structure factor may be written at each temperature as

$$S(\mathbf{q},T)=BS_{cc}(0,T)f(\mathbf{q},T)+A\beta_T[1+0(\mathbf{q})] . \quad (2)$$

The shape of $f(\mathbf{q},T)$ is typically Lorentzian (See Sec. VII); the amplitude is the product of a thermodynamic term $S_{cc}(0)$ which diverges at the critical point

$$S_{cc}(0)=Nk_BT/\left[\frac{d^2G}{dc_2^2}\right]_{T,p} , \quad (3)$$

and a "form factor" or contrast

$$B=\left[\frac{N}{V}\right]^2\frac{[(V_1-V_2)\langle b\rangle-\langle \Delta b\rangle]^2}{\langle b^2\rangle} , \quad (4)$$

or

$$B=\left[\frac{N}{V}\right]^2\frac{(V_1b_2-V_2b_1)^2}{\langle b^2\rangle} , \quad (4a)$$

where V_1 and V_2 are the partial molar volumes of the species.

The sodium-ND_3 system presents one of the largest contrast which may be dreamed of. Indeed the large coherent scattering of the small ND_3 molecule is coupled with the small scattering length of the Na molecule which has a large molar partial volume in solution ($b_1=2.914\times10^{-12}$ cm, $V_1=24.5$ cm^3 for ND_3 and $b_2=0.36\times10^{-12}$ cm, $V_2=68$ cm^3 for Na at −35 °C). Thus $B=6.36$, that is to say fluctuation of concentrations scatter six times more than the homogeneous solution. For example, these values may be compared to those of the isobutyric acid-water system as studied by Schneider *et al.*[10] In this case one finds $B=0.293$, that is to say a factor of 20 in favor of the sodium ammonia system.

The second term of Eq. (2) is expected to vary very slowly with temperature (and with $\mathbf{q}$); indeed β_T is the isothermal compressibility and

$$A=\frac{\langle b\rangle^2}{\langle b^2\rangle}\frac{N}{V}k_BT .$$

From the experimental point of view this term will be included in a q-dependent background with the scattering of the sample environment (container, cryostat, shieldings, window, etc.) and removed from the signal to give the critical corrected spectrum $G(\mathbf{q},T)$.

IV. EXPERIMENTAL

The experiment has been performed on the spectrometer D_{11} at the ILL (Grenoble). A full description of the apparatus may easily be obtained from the ILL. The momentum transfer available ranged between 8×10^{-3} to 5.8×10^{-2} Å^{-1} with the chosen experimental setup ($\lambda=7$ Å and a distance sample detector of 5.6 m). The wavelength resolution $\Delta\lambda/\lambda$ is 0.09 full-width at half maximum (FWHM). Collimation of the incident beam was improved by removing 10 m of the neutron waveguide in front of the sample.

At almost each temperature the experiment has been carried out using successively the upper and lower window. This provided two sets of data which have been treated separately. It was thus possible to detect any temperature gradient (the two centers of diffusion being separated by 15 mm as seen in Fig. 1); indeed the critical scattering is the more sensitive thermometer in the critical region. This procedure had furthermore the purpose to detect a possible concentration gradient induced for example by gravity at the approach of the critical temperature.

Twenty-six runs have been performed at different temperatures between 270 and 241.1 K (the critical temperature); 17 of these were in the nearest degree above T_c. At each temperature the counting had been started 15 min after a good temperature stabilization is reached. Three runs were repeated five or six times to check if this waiting time was sufficient. This repetition allowed to test the

errors (see the data treatment paragraph). The counting time of each run (30–45 min) has been chosen in order to get a relative uncertainty of 0.5% at each scattering angle. Measurements made using the upper window will be referred as experiment I (36 runs if repetitions are included) and those carried out using the lower window referred as experiment II (30 runs; less results than I near the critical point). The high-temperature run, used as a reference to do the background correction, has been carried on during 3 h in order to improve the statistics.

V. CORRECTION FOR INELASTICITY

In evaluating the critical structure factor, the static approximation was assumed to be valid, that is to say a simple relation between the scattering angle and the momentum transfer vector was used,

$$\mathbf{q}=2\mathbf{k}_0\sin\left[\frac{\theta}{2}\right], \tag{5}$$

where $\mathbf{k}_0$ is the wave vector of the incident beam.

This is justified if the energy transfer $\hbar\omega$ due to the scattering is negligible compared to the energy of the incident beam E_0 ($E_0=1.67$ meV for $\lambda=7$ Å). In a normal liquid, the approximation is generally justified at small angle since diffusion coefficients are small; the width of the Raleigh line is $\Gamma=Dq^2$, that is to say the energy transfer $\hbar\omega_{1/2}\approx 2$ μ eV for a typical value of the diffusion coefficient $D=10^{-5}$ cm^2/s and a maximum value of $q=0.07$ Å^{-1}. In the critical region of a binary mixture, the diffusion coefficient is replaced by the mutual diffusion coefficient $D=D_0t^{\nu}$ with $D_0=k_BT\xi_0/6\pi\eta^*$ and Kawasaki equation applies[14]

$$\Gamma=\frac{2}{\pi}Aq^3[x^{-3}+x^{-1}+(1-x^{-4})\arctan(x)], \tag{6}$$

where A is related to D_0, $A=3D_0\xi_0/8$.

Most of the delicate data treatments leading to the evaluation of the critical index η (which is small) have been carried out in the critical regime ($x>1$ and $T-T_c<0.5$ K). Correction problems must be considered in this region with a particular attention. The large x limit of 6 is $\Gamma=Aq^3$. The mutual diffusion coefficient is not known in the sodium ammonia system but the error would not be underestimated by using for D_0 the diffusion coefficient of each species which is of the order of 6×10^{-5} cm^2/s.[15] Then the critical energy transfer, which does not depend on ξ or T near T_c, is $\hbar\omega_{1/2}=0.9$ μeV at $q=0.07$ Å^{-1}. In the hydrodynamic regime, the less-favorable situation is found for large q and small ξ. For example, for $\xi=15$ Å and $q=0.007$ Å^{-1} ($x\approx1$), one finds $\hbar\omega_{1/2}=1.15$ μeV. If the average energy transfer $\langle\hbar\omega\rangle$ is of the order of $\hbar\omega_{1/2}$ then deviations from Eq. (5) never exceed 3.5×10^{-5} Å^{-1} and the static approximation is well justified in the whole temperature range.

VI. RAW DATA HANDLING AND BACKGROUND EVALUATION; THE CORRECTED INTENSITY

On the D_{11} spectrometer, data are collected on a two-dimensional multidetector (64×64 cells of 1 cm^2 each). Since the diffusion is centrosymmetric, the data are regrouped to get a one-dimensional pattern $I=f(r)$, r being the distance from the center of diffusion. The momentum transfer q is then written

$$q=\frac{4\pi}{\lambda}\sin\left[\arctan\left[\frac{r}{2d}\right]\right], \tag{7}$$

where d is the distance between the sample and the detectors plane. All this delicate first stage data treatment has been performed using the program package provided by Ghosh[16] (i.e., finding the center of diffusion, removing cells perturbed by the central beam stop, checking the symmetry of the patterns, and regrouping). Data were then corrected for the detector efficiency which has been determined, as usual, from the diffusion of a water sample.

The measured scattering cross section is in fact an addition of several contributions: critical scattering; incoherent scattering, q independent, which is mainly due to the H and D atoms of the ammonia molecules; coherent scattering from the structure factor of the mixture; scattering from the quartz windows and copper shieldings of the sample environment.

The more precise way to extract the critical scattering from raw data is to subtract from each run a "high-temperature run" for which the critical scattering is weak or negligible. The temperature of the reference run is 274 K ($T_{\rm ref}-T_c=33$ K). At this temperature, the critical scattering is not completely negligible (from previous experiments, the correlation length should be of the order of 15 Å). The reference critical scattering may be evaluated by a four-parameters least-square fit performed on the difference of intensity observed between two scattering patterns using the Ornstein-Zernlike equation

$$I-I_{\rm ref}=\frac{a}{1+q^2\xi^2}-\frac{a'}{1+q^2\xi'^2}. \tag{8}$$

In this calculation all contributions beside critical scattering were supposed to be temperature independent. As previously indicated,[17] a' is not expected to be equal to a since contribution from the structure factor and the compressibility may no longer be neglected in front of the critical scattering at small correlation length.

The fit is performed using all runs with $T_{\rm ref}-T>10$ K. The value of ξ' evaluated from 43 runs (using the upper and lower window) is 15.7 ± 0.3 Å. The background may then be evaluated by subtracting the critical contribution from the reference run. As a check, it is found that the remaining intensity left by subtracting the signal of the empty cell and cryostat (corrected for transmission) from the background is q independent; that is expected if the remaining intensity is due to the incoherent scattering and the structure factor which is flat for $q<0.4$ Å^{-1} far from the critical temperature [second term of Eq. (2)]. Since the amount of solution in the irra-

diated volume is slightly temperature dependent (as density), the intensity of a "working background" corrected for density has been evaluated at each temperature using data of Kraus *et al.*[18] That defines the corrected intensity $I(q,T)=I_{\rm obs}-I_B(q,T)$.

VII. FORMALISM

For a binary mixture on the critical isochore, the corrected intensity is proportional to the critical scattering function

$$I(q,T)\propto G(q,T)=t^{-\gamma}g(q\xi)\ , \tag{9}$$

where t is the reduced temperature $t=T/(T-T_c)$, T_c is the critical temperature, γ is the critical index related to the divergence of $G(0,T)$, $g(q,\xi)$ is the critical scaling function [a scaled form of $f(\mathbf{q},T)$ in Eq. (2)]; and ξ is the correlation length which diverges as $\xi=\xi_0 t^{-\nu}$. Scaling predicts that

$$\gamma=\nu(2-\eta)\ , \tag{10}$$

where η is a critical index introduced by Fisher.[6] As shown by Aharony and Fisher,[1] the critical scaling function satisfies the two limit conditions

$$g(x)_{x\to 0}=D_0(1+x^2)^{-1}\ , \tag{11}$$

$$g(x)_{x\to\infty}=D_\infty x^{-2+\eta} \tag{12}$$

with $x=q\xi$. In three-dimensional systems, $D_0=1$ and $D_\infty\approx 0.90$.

One of the main problems is to determine the critical index η which governs the shape of the scattering function at large x. There may be two experimental ways of determining η. The first one is to compare the divergence of the correlation length ξ with that of the thermodynamic function $G(0,T)$; one thus gets the corresponding critical indices ν and γ, and η may be calculated from scaling; but the value of η is very small (less than 0.10) and the experimental uncertainty found on the indices ν ($\sim 0.63\pm 0.02$) and γ ($\sim 1.24\pm 0.02$) leaves little hope of finding a precise value of η by this method. The second, more promising way is to study the shape of the scattering function $g(x)$ in the intermediate and large x range.

There is no analytical equation or exact numerical results to describe the scattering function between the two limits [Eqs. (11) and (12)]. Several approximate equations have been discussed in the literature. Equations (13)–(16) are some of the more useful approximations:

Ornstein-Zernike(OZ) ,

$$g_{\rm OZ}(x)=a_{\rm OZ}(1+q\xi^2)^{-1}\ ; \tag{13}$$

Fisher ,

$$g_F(x)=a_F(1+x^2)^{-1+\eta/2}\ ; \tag{14}$$

Fisher-Burford (FB) ,

$$g_{\rm FB}(x)=a_{\rm FB}(1+\phi^2x^2)^{\eta/2}(1+x^2)^{-1}\ , \tag{15}$$

and Fisher-Langer (FL) ,

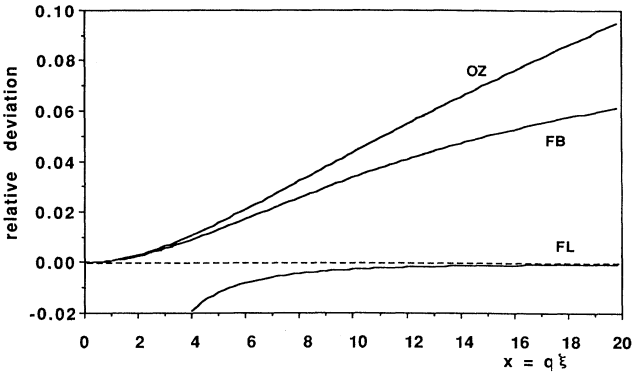

FIG. 2. Deviations of approximate equations Ornstein-Zernlike (OZ), Fisher-Burford (FB), and Fisher-Langer (FL) from the exact value of the scattering function in two dimensions. The data are from Tracy and McCoy (Ref. 3).

$$g_{\rm FL}(x)=C_1(1+C_2x^{(1-\alpha)/\nu}+C_3x^{-1/\nu})x^{-2+\eta}\ . \tag{16}$$

The validity range of these equations has been studied in the two-dimensional Ising model by Tracy and McCoy;[3] deviations between the estimations and the exact values which may be obtained numerically in this particular case are reported in Fig. 2. Deviation less than 1% is found with OZ for $x<4.0$, Fisher for $x>1170$, FB for $x<4.2$ and $x>1145$, FL for $x>5.4$ and for $x>1170$ with the large-x limit [LX, Eq. (12)].

In three dimensions there are no exact values of $g(x)$ available; nevertheless a "best estimation" has been proposed by Bray[4] from a dispersion-theory approach with the asymptotically exact Fisher-Langer equation used as a base. The agreement found with the exact value of the 2D Ising model is better than 0.03% in the whole x range; the agreement with the exact values found in four dimensions is also good. Then the values calculated in 3D, which agree with the results of high-temperature series expansion and with ϵ expansion, may be used as the more reliable approximations. Deviations between the approximate equations and the results of Bray (using $\nu=0.638$, $\alpha=0.125$, and $\eta=0.041$) are reported in Fig. 3. Validity ranges of the approximations are more ex-

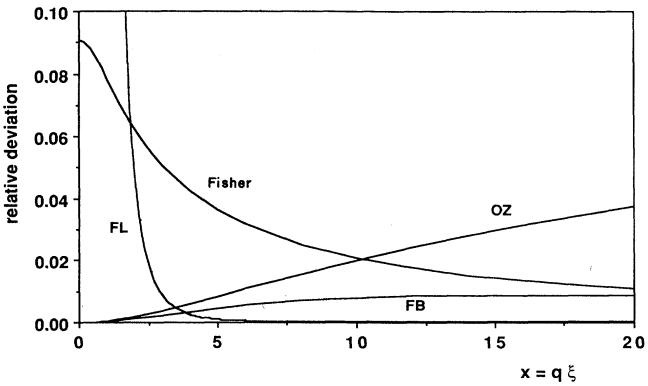

FIG. 3. Deviations of approximate equations [same as in Fig. 2 plus Fisher from the "best estimate" proposed by Bray (Ref. 4)]. The validity range (deviation less than 1%) is more extended in three dimensions than in two dimensions.

tended in 3D than in 2D. A 1% deviation is found with OZ for $x<5.7$, Fisher for $x>22$, FB for $0<x<\infty$, FL for $x>3$. In summary, the FB equation should be a rather good approximation in the whole x range and there exists a large overlap (inside the 1% deviation limit) between the more exact FL equation at large x and the small-x range approximations OZ or FB. The Fisher approximation is simpler than FL, but it will be of limited use since its validity falls almost out of experimental reach.

From the practical point of view, a judicious choice of the equation and of the number of parameters to be fitted must be made depending of the x range investigated. In the small-x range, data are rather insensitive to the value of the index η and OZ formalism may be used with the fitted parameters $a_{OZ}\equiv D_0$ and ξ. At large values of $x=q\xi$, the FL equation will be used, but the independent variable must then be x and not q, as with OZ, and the correlation length must be previously determined (from light scattering as done by Schneider *et al.*[10] or from a SANS experiment performed at small x). The FL equation has six unknown parameters which cannot be fitted from a set of data obtained by SANS. It will be seen in Sec. VIII that only two parameters $C_1\equiv D_\infty$ and η may be fitted with significance using FL (or three parameters C_1, η, and C_2 in the more favorable cases). The index ν is taken from theory ($\nu\approx 0.635$) or determined from the temperature dependence of ξ; the index α is taken from theory (for example $\alpha=0.125$) and C_2, C_3 will be generally taken from theory (Bray[4]).

In the FB equation, the value of the constant ϕ is imposed by boundary conditions. It is easily shown that from the $x\to 0$ limit $a_{FB}=a_{OZ}=D_0$ and that $a_{FB}\phi^\eta=C_1=D_\infty$ in the $x\to\infty$ limit. This equation will prove itself to be very useful since it is a good approximation in the whole range and since the correlation length may be one of the fitted parameters together with D_0, C_1, and η.

The corrected intensity is proportional to $G(x)$ from Eqs. (2) and (9). At $q=0$, $G(0)=t^{-\gamma}$. Since an absolute determination of $S_{cc}(0)$ is not the object of this paper we will write $G(0)=S_{cc}(0)=t^{-\gamma}$, omitting a normalization factor.

VIII. DATA ANALYSIS

All the equations used in the data analysis, excepted OZ, need nonlinear least squares. Procedures proposed by Press *et al.*[19] have been used in most of the cases. Depending on the fitted equation, the algorithms may be adapted to converge rapidly.

Theoretical uncertainties are easily evaluated in neutron scattering experiments (typically $\Delta N=\sqrt{N}$). Great care has been taken to introduce correctly the errors in the fitting procedures. The first important use is to allow the proper weighting factor to each data point. Then the error on each parameter and correlation between parameters may be determined. Since absolute uncertainty may be evaluated, a goodness of the fit test (G_f) was made using the complement of the incomplete Γ function $G_f=Q(\nu/2,\chi^2)$, where ν is the number of degrees of freedom and χ^2 the minimized "chi square." If a value of G_f laying, say, between 0.05 and 0.5 is found, then the dispersion of the sampled data is in the same range as theoretical errors (based on an infinite sample) and the chosen function is probably a good representation of the observations.

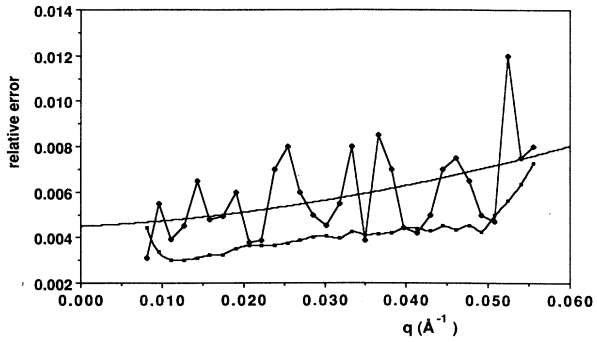

FIG. 4. Standard deviations of the intensity observed for a run repeated six times, ($T-T_c=0.350$ K), ◆, and calculated error ($\Delta I=\sqrt{I}$), ■, as a function of the momentum vector transfer q. The observed dispersion of data is about 40% larger than that evaluated from statistical uncertainty only. The same behavior was observed for two other runs repeated six and five times.

In fact, it was found that observed dispersion was systematically somewhat larger than evaluated from statistical error only. Different reasons may be invoked: the statistical error does not account for temperature uncertainty, fluctuations of the neutron beam average wavelength, electronic noise, etc. To get a realistic evaluation of the errors, three runs have been repeated 5 or 6 times; for a set of data, the dispersion of data were on average 40% larger than calculated; there was no marked dependence of the 1.4 ratio with the diffusion angle (Fig. 4) or temperature. For each data point, the evaluated error was then chosen as $1.40\sqrt{I}$. This calibration does not affect the fitting procedure itself and then the values of the parameters, but only the χ^2, and then G_f and the calculated uncertainty of the parameters.

IX. DETERMINATION OF THE CORRELATION LENGTH AND $S_{cc}(0)$

A. Ornstein-Zernike equation

The OZ equation is the best to determine the correlation length ξ and $S_{cc}(0)$ at each temperature from data collected in the low $q\xi$ range. In order to respect the validity range as discussed in the preceding paragraph, a two-step procedure has been followed; a first calculation using all data gave a first evaluation of ξ; then only data for which $q\xi<$ limit were kept in the second calculation (the limit is $q\xi<5.7$ if an error of 1% is allowed). This fit may not be used for values of ξ larger than 300 Å with the chosen experimental setup since too many of the data are then rejected. For large values of ξ (250–300 Å), the 1% error limit may also be questioned (see Fig. 5).

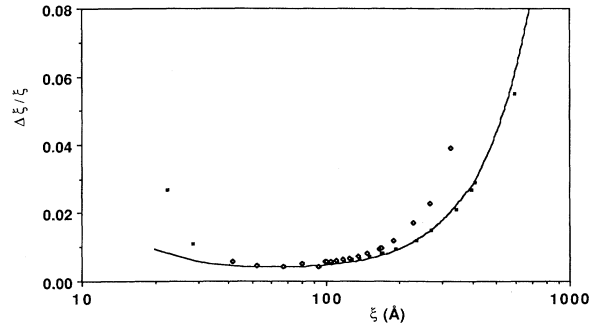

FIG. 5. Relative uncertainty of the correlation length $\Delta\xi/\xi$ as a function of ξ, ◇ for Ornstein-Zernike equations and ■ for Fisher-Burford equations. The solid curve is the error found for simulated experiment with a Gaussian random error (FB). The uncertainty calculated for COZ is similar to that of FB and is not reported here.

B. Extended Ornstein-Zernike (EOZ) equation

As shown by Tracy *et al.*[3] in two dimensions, the validity range of the OZ formalism may be somewhat extended if a first correction to the Lorentzian shape at large x is used,

$$g(x)=a_{\mathrm{OZ}}(1+x^2-Bx^4)^{-1}\ , \tag{17}$$

with $B=\Sigma_4$ of Ref. 3. In two dimensions the validity range (for 1% error) is then extended from $q\xi=4.2$ to 6.6; from a simulated experiment, we found that the limit could be extended to $q\xi=10$ in three dimensions. Values of ξ up to 400 Å may then be determined with a good precision.

C. Fisher-Burford equation

The correlation length and $S_{cc}(0)$ may alternatively be determined from the FB equation without range restraint (in the 1% error limit). Three parameters were fitted, $S_{cc}(0)$, η, and ξ, using $\phi=C_1^{1/\eta}$. The value of C_1 was chosen as 0.91 from OZ data treatment at low x and Fisher at large x; indeed, $C_1=a_F(x\to\infty)/a_{\mathrm{OZ}}(x\to 0)$ from Eqs. (11)–(16). This value is in good agreement with theoretical evaluations [C_1 ranging from 0.89 to 0.92 (Ref. 4)]. The calculated values of ξ will be reliable if the values of η determined at the different temperatures are not dispersed; more precise values of ξ are then calculated using the average value of η as a constant.

D. Fully corrected Ornstein-Zernike (COZ) equation

Finally a fourth way of determining the correlation length and $S_{cc}(0)$ was to take the "best estimate" proposed by Bray as a reference (referred to as Bray). Then the deviation of the OZ equation (Fig. 2) may be fitted to a polynomial $\sum a_n x^n$. For x ranging from 0 to 20 an excellent fit was found with $a_0=a_1=0$, $a_2=5.667\times10^{-4}$, $a_3=-5.796\times10^{-5}$, $a_4=2.576\times10^{-6}$, and $a_5=-4.299\times10^{-8}$, the standard deviation of the estimates being 5.8×10^{-5}. The data may then be treated using this correction with the OZ equation

$$g_{\mathrm{COZ}}(x)=a_{\mathrm{OZ}}(1+x^2)^{-1}\Big/\left[1-\sum_{n=2}^{5}a_n x^n\right] \tag{18}$$

with a_{OZ} and ξ being the fitted parameters. The same results are obtained for x ranging from 0 to 40 if two additional terms a_6 and a_7 are used in the fit. These coefficients are empirical; there are no odd values of n in the power-series expansion for small x (see Bray[4]) but the present empirical expansion may be used at large values of x. This last method could well give the best results; the limit is that it is based on a "best estimation" of $g(x)$ and not exact values; several parameters, $\alpha=0.125$, $\nu=0.638$, $\eta=0.041$, and $C_2+C_3=-0.9$, are already included in the model.

E. Results

The four methods give essentially the same results for $\xi<300$ Å; FB give slightly larger values at large ξ (1–3 % at the limit of the error bar); a comparison of the methods is given in Table I for three different values of ξ.

TABLE I. Comparison of the correlation length ξ obtained with four fitting equations [(13), (17), (15), and (18)] for three different runs.

	$T-T_c$ (K)	ξ (Å)	$\Delta\xi$	Number of data points	Goodness of the fit G_f
OZ	0.725	109.51	±0.74	24	0.065
EOZ		109.96	±1.07	30	0.15
FB		110.47	±0.71	30	0.18
COZ		110.18	±0.72	30	0.70
OZ	0.355	166.88	±1.73	13	0.061
EOZ		166.43	±1.88	30	0.108
FB		167.96	±1.37	30	0.137
COZ		166.90	±1.41	30	0.155
OZ	0.127	325.73	±12.7	7	0.046
EOZ		333.68	±14.0	14	0.041
FB		334.22	±6.9	30	0.42
COZ		326.14	±7.8	30	0.35

The reproducibility (several runs carried out at the same temperature) and comparison between experiment I (36 runs with 19 in the nearest half degree from T_c using the upper window) and experiment II (30 runs with 12 in the nearest half degree from T_c using the lower window) have been carefully checked. For example, a run at $T \approx 241.462$ K has been performed six times, giving $\xi = 168.03 \pm 1.44$, 168.29 ± 1.43, 168.65 ± 1.44, 167.66 ± 1.43, 166.59 ± 1.42, and 166.90 ± 1.4 Å ($\langle \xi \rangle = 167.69$ Å, $s = 0.81$ Å). From the lower window, $\xi = 167.01 \pm 1.58$ Å. There is no systematic deviation between experiments I and II (the difference exceeds two times the standard error only twice). This observation is encouraging since all the steps of the data treatment for experiments I and II are carried out in completely independent ways.

Figure 6(a) reports a few examples of experimental data and fitted curves (COZ equation); it shows the increase of the diffuse intensity at small angles when the critical temperature is approached. From this figure, the quality of the fits looks "good." In fact, it is not really possible to draw any conclusion about the fits from this kind of plot since the predicted error on each data point is about 0.5%. A more quantitative approach of the goodness of fits is given in Fig. 6(b); it reports the observed residual I_{calc}-I_{obs} divided by the calculated standard error for a typical run ($T - T_c = 0.23$ K and

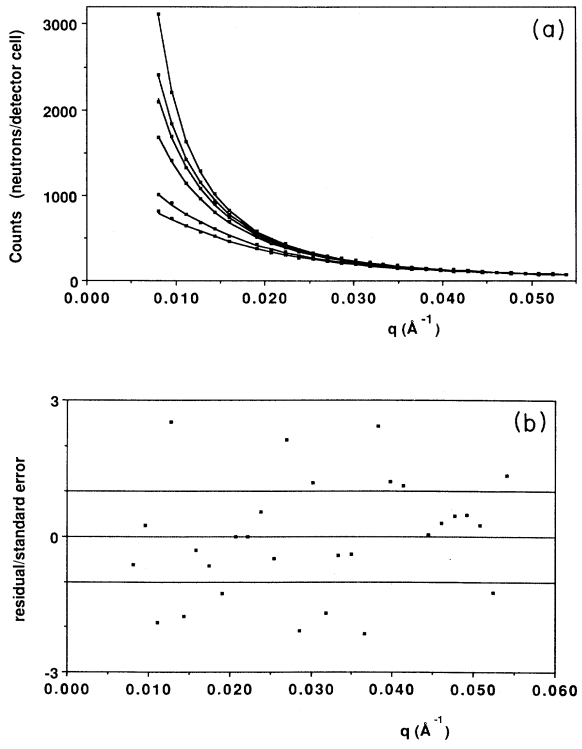

FIG. 6. (a) A few examples of calculated (solid lines) and experimental (■) results; values of $T - T_c$ are, respectively (from bottom to top), 1.68, 1.28, 0.58, 0.23, and 0.04 K. (b) Residual over calculated standard deviation for a typical run as a function of q; the goodness of the fit G_f was equal to 0.19 and $T - T_c = 0.23$ K.

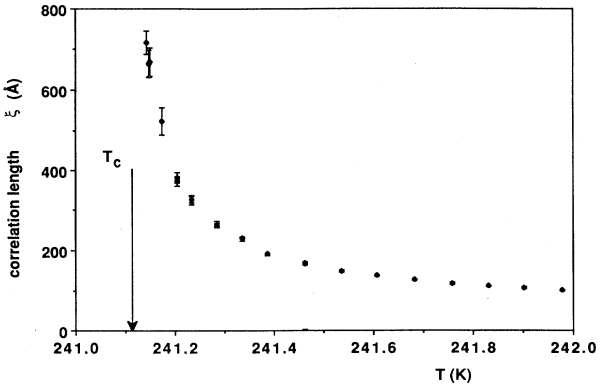

FIG. 7. The correlation length ξ as a function of temperature in the nearest degree from T_c (experiment I). It was not possible to calculate the correlation length for two runs very near T_c.

$G_f = 0.19$). This figure tells that there is no visible trend for the deviation as a function of q. The fit presented in this figure is really a typical one (and not the best). For any of the equations used in its validity range, values of G_f between 0.10 and 0.80 were found for 48 runs (out of 53 runs for which $\xi > 65$ Å) and values larger than 0.025 for the remaining five runs; three of these five runs have large values of ξ, that is to say a large counting rate and then a low calculated relative error on the counting. In these cases the precision was no more completely limited by the statistics but also by the quality of the detector calibration and of the temperature stabilization. Finally it was not possible to determine the value of ξ for the two runs closest to T_c ($\xi > 750$ Å).

The values of the correlation length obtained for experiments I and II are reported in Fig. 7. Since they are not absolute values, results of $S_{cc}(0)$ are not given here but they will be used in Sec. X to determine the critical index γ.

X. DETERMINATION OF THE CRITICAL INDICES ν, γ, and η

At the approach of the critical point, on the critical isochore, the correlation length ξ diverges following a power law

$$\xi = \xi_0 \left[\frac{T}{T_c} - 1 \right]^{-\nu} . \tag{19}$$

If the concentration is not exactly the critical one, the critical temperature is replaced in (19) by the spinodal temperature T_s and a gap exists between the temperature of the coexistence curve and T_s, preventing critical divergence to fully develop. From all the observations of the counting rate just above and below T_c for the two experiments, the critical temperature may be evaluated at 241.107 K (not an absolute scale); it may also be asserted that T_c (or T_s) is below 241.110 K. A lower limit should not be less than 241.100 K even if the evaluation of the gap is less sure. The evaluated value of the critical temperature could then be used in Eq. (19) to determine ξ_0

and ν. It was found that it would better let the critical temperature be adjusted together with ξ_0 and ν and to reconsider results with T_c outside the above range. Determination of T_c from a least-squares fit is difficult; all data with large values of ξ, which should determine T_c with the best precision, have at the same time large relative errors and then weigh very little in the fit. In the present case the problem is somewhat complicated by the existence of a crossover between critical ($\nu=0.63$) and classical regime ($\nu=0.50$) at about 1° above T_c.[20]

The recipe was the following. Three tests provide information to improve the fit when all data are first used in a three-parameter fit (25 data with $\xi>90$ Å in experiment I): (i) the value of G_f (here $G_f=5.9\times10^{-3}$); (ii) value of T_c compared to the above range (here $T_c=241.117$ K, i.e., 0.007 K above the higher limit); (iii) inspection of residues which shows that evaluated values of ξ for $\xi>450$ Å are larger than that observed (out of the error bar but their weight is low). The value of ν is equal to $0.577\pm6.5\times10^{-3}$. Data from the low-ξ range (high temperature) are then rejected one by one from the fit; one then observes that T_c decreases, G_f is improved, and large ξ evaluations reenter into the error range. The best fit is obtained when data ranging from $T-T_c=0.50$ to 0.03° ($140<\xi<700$ Å) are used in the fit (16 points). Then $T_c=241.1050\pm0.0043$ K, $\nu=0.644\pm0.022$, $\xi_0=2.66\pm0.36$ Å with $G_f=0.19$; if one point with a ratio of residual/error equal to 2.8 is removed, the following values are found: $T_c=241.1078\pm0.0040$ K, $\nu=0.622\pm0.021$, $\xi_0=2.89$ Å with $G_f=0.70$. No systematic trend is found by removing other data and values of the index ν remains in a range 0.605–0.655 with larger error bar. From all fits [divergence of ξ and $S_{cc}(0)$ for the two experiments], it is found that the value $T_c=241.1075$ K is a good evaluation; it finally gives $\nu=0.6279\pm0.008$, $\xi_0=2.788\pm0.15$ Å with $G_f=0.80$. There is no systematic variation of the index ν by removing data from $\xi=120$ Å (19 points) to $\xi=400$ Å (five points) if T_c is held constant (241.1075 K); an average value $\langle\nu\rangle=0.631$ is found with a standard deviation $s=0.009$. This small dispersion is coherent with the high value of G_f obtained in the fits. At the two limits the index ν is equal to 0.616 for $T_c=241.11$ K ($G_f=0.56$) and 0.661 with $T_c=241.100$ ($G_f=0.23$). In this last case the third test (iii) is not fulfilled.

It is more difficult to use the same procedure with experiment II since the set of data is less complete (less data in the vicinity of the critical point). With ten values in the same temperature range, one finds $T_c=241.1073$ K and $\nu=0.609\pm0.032$ ($G_f=0.03$); with constant T_c (241.1075 K from experiment I), the index ν is equal to 0.613 ± 0.032 ($G_f=0.03$).

In the same way, the critical index γ may be determined from the power law

$$S_{cc}(0)=C_0\left[\frac{T}{T_c}-1\right]^{-\gamma}, \tag{20}$$

where C_0 is a non-normalized constant as already indicated.

Using the same set of data as for the determination of the index ν, one finds

$\gamma=1.228\pm0.039$, $T_c=241.1086\pm0.0043$ K, and $G_f=0.72$;

$\gamma=1.240\pm0.0157$, $G_f=0.79$ with $T_c=241.1075$ K (experiment I) ;

$\gamma=1.223\pm0.019$, $G_f=0.03$ with $T_c=241.1075$ K (experiment II) .

From this, the index η may be calculated if the scaling laws are accepted. Then, with $T_c=241.1075$ K, one finds from experiment I

$$\eta=2-\frac{\gamma}{\nu}=0.025 . \tag{21}$$

The good agreement with theory and with the values that will be obtained using data in the large-x range (Sec. XI) is fortuitous if one considers the errors. Indeed, if the errors made on γ and ν are not linked, one obtained an uncertainty of ±0.052 on η from the errors found on ν and γ and Eq. (21). But the uncertainties are probably somewhat linked [indeed the value of Eq. (21) remains almost unchanged when T_c is changed in Eqs. (19) and (20) from 241.10 and 241.11 K]. This may be checked by considering another form of the OZ (or FB, EOZ, and COZ) equation:

$$I\propto t^{-\gamma}(1+q^2\xi^2)^{-1}=t^{\eta\nu}\left[\frac{1}{\xi^2}+q^2\right]^{-1} \tag{22}$$

from Eqs. (9) and (10).

All the calculations made in Sec. IX are then made again with these modified equations. They give the same values of the correlation length and a new parameter a_1 which varies little with temperature ($\eta\nu\approx0.02$). The values of a_1 are reported in Fig. 8 as a function of temperature. The value of $\eta\nu$ may be obtained from a power law

$$a_1=Ct^{\eta\nu} . \tag{23}$$

From the best set of data (experiment I, 16 points) one finds $\eta\nu=0.0177\pm0.0029$ and $T_c=241.1033$ K. The critical temperature is not well defined in experiment II ($T_c=241.13$ and $\eta\nu=0.0152$ from 10 points). With constant $T_c=241.1075$ K, one obtains $\eta\nu=0.0178\pm0.0007$,

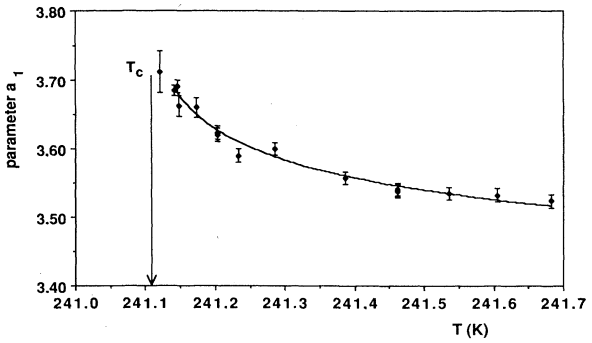

FIG. 8. Parameter a_1 [Eq. (23)] as a function of temperature. The slow divergence ($t^{\eta\nu}$) is clearly observed very near the critical point.

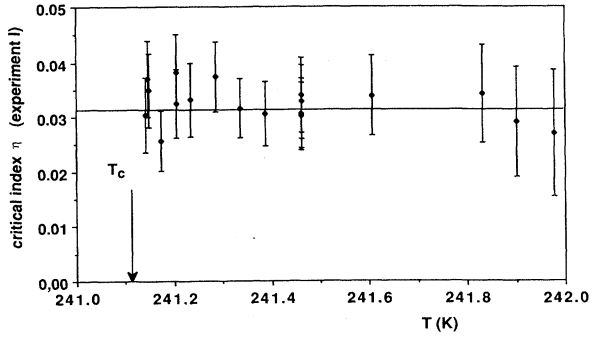

FIG. 9. The critical index η obtained from Fisher-Burford [Eq. (15)] and Eq. (9) for experiment I. The average value is $\eta=0.0317$ and the standard deviation $s=0.0051$; the average of the standard error given by the fits is 0.0065.

experiment I; $\eta\nu=0.0165\pm0.0014$, experiment II. With $\nu=0.628$, the value of the index η is then equal to 0.0283 (experiment I) with an unexpected low standard deviation of 0.002 (and 0.026 ± 0.004 from experiment II).

XI. A STUDY OF THE SCATTERING FUNCTION $G(q,T)$ AT LARGE x: DETERMINATION OF THE CRITICAL INDEX η

As seen in Sec. VII, FB and FL equations are good approximations of the scattering function in the intermediate- and high-x range. They are applied here to determine the shape of the scattering function $G(q,T)$ and to evaluate the critical index η.

In a first step, the FB approximation is applied on each run covering a limited x range at constant ξ. A FB fit [Eqs. (9) and (15)] with three unknown parameters $S_{cc}(0)$, ξ, and η is applied to each run with a constant $C_1=0.91$ (Sec. IX). The values of $S_{cc}(0)$ and ξ have been discussed in Secs. IX and X. The values of η obtained from experiments I and II are reported in Figs. 9 and 10, respectively. The averages are $\langle\eta\rangle=0.0317$, $s=0.0051$ for experiment I (22 points) and $\langle\eta\rangle=0.0305$, $s=0.0091$ for experiment II (15 points). The average of the standard errors given by the fits are, respectively, 0.0065 and 0.0061.

Then all data which were functions of q and T are regrouped as a function of the single variable $x=q\xi$ and the approximate equations are used to determine the scaled scattering function $g(x)$ and a more precise value of the index η. That is achieved by using scaling and values of ξ and $S_{cc}(0)$ calculated in Sec. IX. Normalized values of $g(x)$ (method *a*) are obtained by dividing the observed count rate by $S_{cc}(0)$ [Eqs. (9) and (20)]; but a non-normalized form (method *b*), where $t^{-\gamma}$ is replaced by $\xi^{2-\eta}$ in Eq. (9), could be preferred since it was found that errors made on ν and γ [or ξ and $S_{cc}(0)$] were linked. Two sets of data (experiments I and II) are thus built from results obtained in the $140<\xi<700$ Å range.

The results obtained from the fit using FL, FB, and LX [Eq. (12)] equations are reported in Table II. The data set (experiments I or II), the number of data used in the fit (a maximum of 350), and the type of equation (FL or FB, method *a* or *b*) are reported in columns 1 and 2. The calculated values of the fitted parameters, their standard error, and the goodness of the fit are reported in columns 3, 4, and 5, respectively, and the conditions of the fit ($q\xi$ range, parameters introduced as constants) are given in column 6. Most of the reported results are from the more complete set of experiment I, but, as already found in the previous sections and as shown in a few examples, the fitted parameters obtained from the two experiments are not significantly different.

The results obtained with the FB equation are reported first (fits 1–6). As a starting point, method *b* is used with C_1 held constant ($C_1=0.91$ as found with the Fisher equation at large x); the variable $x=q\xi$ has been calculated from experimental values of ξ obtained in Sec. IX. The effect of varying C_1 is shown in fit 2; a general observation is that a 1% decrease of C_1 increases the index η by 2×10^{-3}. Since the set of data is very large, it is in fact possible to determine C_1 with a good accuracy (fit 3). The x range may be extended using calculated values of the correlation length (see Sec. X); two runs close to T_c are then included in the data set (fit 4). Fits 5 and 6 use a normalized $g(x)$ obtained by dividing the corrected intensity by the values of $S_{cc}(0)$ calculated in Sec. IX (method *a*). As a short conclusion, it may be noticed that

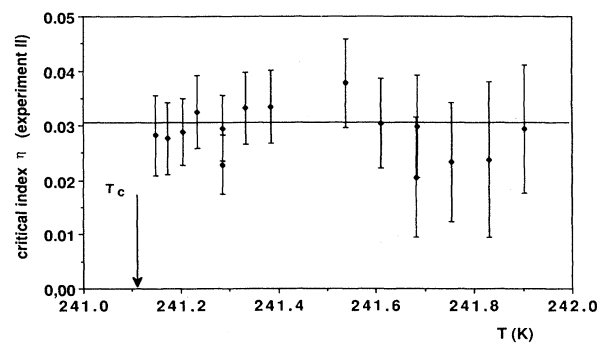

FIG. 10. Same as Fig. 9 for experiment II. The average value of η is 0.0305, $s=0.0091$ and the average of the standard deviation given by the fits is 0.0061.

TABLE II. Parameters which define the shape of the scaled function $g(q\xi)$ using Fisher-Burford and Fisher-Langer equations. A complete description of the fits is given in the text. From FL, the value of the index η is 0.0305 ± 0.0015 without assuming scaling and 0.0286 ± 0.0010 using the scaling hypothesis [Eq. (10)]; a value close to 0.028 was found from scaling only (Sec. X). The difference is at the limit of significance. The scaling hypothesis is then verified within the limit $2-\eta-\gamma/\nu \leq 0.002$.

Fit number, experiment, equation	Number of data points	Fitted parameters	Standard error	Goodness of the fit G_f	Conditions of the fit, constants
1, I, FB(b)	350	$\eta=0.0284$	0.00077	0.72	$1.1<q\xi<37$ $C_1=0.91$
2, I, FB(b)	350	$\eta=0.0304$	0.00075	0.70	$1.1<q\xi<37$ $C_1=0.90$
3, I, FB(b)	350	$\eta=0.0283$ $C_1=0.9119$	0.0018 0.0025	0.75	$1.1<q\xi<37$
4, I, FB(b)	350	$\eta=0.0288$	0.00077	0.54	$0.1<q\xi<66$ $C_1=0.91$
5, I, FB(a)	350	$\eta=0.0289$ $a_{FB}=1.00083$ $C_1=0.906$	0.0011 0.0027 0.053	0.74	$0.1<q\xi<66$
6, II, FB(a)	205	$\eta=0.0280$ $a_{FB}=1.00014$ $C_1=0.907$	0.0046 0.002 0.10	0.45	$0.1<q\xi<37$
7, I FL(b)	276	$\eta=0.0281$	0.0011	0.10	$4<q\xi<49$ $C_2=1.845$ $C_3=-2.745$ $\nu=0.632$ $\alpha=0.110$
8, I, FL(b)	276	$\eta=0.0284$ $C_2=1.852$ $(C_2+C_3=-0.897)$	0.0009 0.0037	0.033	$4<q\xi<49$ $C_3=-2.745$ $\nu=0.632$ $\alpha=0.110$
9, II, FL(b)	205	$\eta=0.0286$ $C_2=1.885$ $(C_2+C_3=-0.860)$	0.0017 0.0023	0.062	$4<q\xi<32$ $C_3=-2.745$ $\nu=0.632$ $\alpha=0.110$
10, I, FL(b)	350	$\eta=0.0285$ $C_2=1.906$	0.0010 0.017	0.63	$4<q\xi<66$ $\nu=0.628$ $\alpha=0.110$ $C_2+C_3=-0.90$
11, I, FL(b)	350	$\eta=0.0282$ $C_2=1.524$ $C_2+C_3=-0.79$	0.0009 0.10 0.026	0.54	$4<q\xi<66$ $\nu=0.628$ $\alpha=0.110$
12, I, LX(a)	154	$\eta=0.0319$ $C_1=0.929$	0.053 0.021	0.26	$10<q\xi<49$ $\nu=0.632$ $\alpha=0.086$
13, I, FL(a)	276	$\eta=0.0302$ $C_1=0.937$ $C_2=1.892$ $(C_2+C_3=-0.853)$	0.0011 0.006 0.030	0.17	$4<q\xi<49$ $\nu=0.632$ $\alpha=0.086$ $C_3=-2.745$
14, I, FL(a)	276	$\eta=0.0305$ $C_1=0.939$ $C_2=2.630$	0.021 0.021 0.76	0.10	$7<q\xi<49$ $\nu=0.632$ $\alpha=0.086$ $C_2+C_3=-0.90$
15, I, FL(a)	334	$\eta=0.0308$ $C_1=0.933$ $C_2+C_3=-0.828$	0.019 0.005 0.030	0.33	$4<q\xi<66$ $\nu=0.628$ $\alpha=0.11$ $C_2=1.845$
16, II, FL(a)	175	$\eta=0.0324$ $C_1=0.932$ $C_2=1.944$ $(C_2+C_3=-0.801)$	0.046 0.012	0.020	$4<q\xi<32$ $\nu=0.628$ $\alpha=0.11$ $C_3=-2.745$

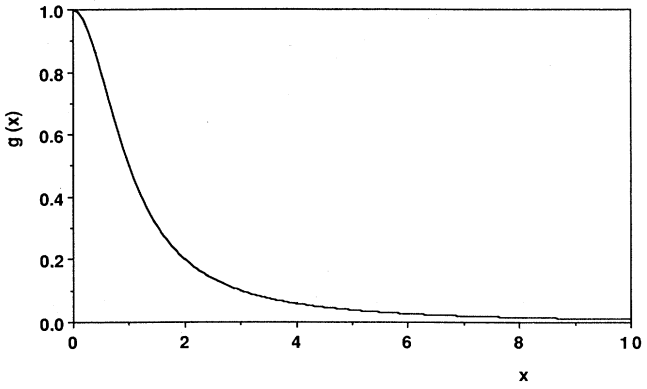

FIG. 11. Function $g(x)$ obtained from parameters of fit 5 (Table II) in the 0–5 x range using the FB equation and fit 11 (Table II) in the 4–10 x range with the FL equation.

the value of the index η is found between 0.028 and 0.029 with a high precision (≈ 0.001); the value of C_1 is near 0.91; experments I and II and methods a and b give essentially the same results.

Fisher-Langer or LX (LX is equivalent to FL with $C_2=C_3=0$) approximations have been used in the other fits (7–16). Fits 7 and 8 for experiment I and 9 for experiment II are performed with C_2 and C_3 or only C_3 held constant. Indices ν and α are those of renormalization theory.[5] In fit 10 the x range is extended as in fit 3, the index ν is that calculated in Sec. X, and the sum C_2+C_3 is imposed; indeed, if the values of the coefficients C_2 and C_3 may not be well evaluated from theory, a value $C_2+C_3=-0.90$ seems more sure.[4] This value is not far from that found in fits 8 and 9 where one of the two parameters is held constant. Nevertheless fit 11 shows that the sum is -0.79 if one tries to calculate both C_2 and C_3. The index η shows a remarkable stability when C_2 and C_3 and even ν are varying using FL(b) ($\eta=0.0286\pm0.0010$).

A value of η somewhat larger (0.0319) but with a large uncertainty is found with the LX equation ($x>10$); the parameter C_1 is 2% larger than with the FB (or Fisher) equation but again with a large uncertainty ±0.021 (fit 12).

The FL(a) equation is finally used in fits 13–16 with different combinations and values of C_2, C_3, α, and ν. Again the index η is very stable but the average value is about 0.002 larger than with method b, but as expected, the errors are greater. As with LX, the parameter C_1 is near 0.935.

A plot of the function $g(x)$ obtained by a superposition of fits 5 and 11 (Table II) is reported in Fig. 11.

XII. DISCUSSION

Results presented in Secs. IX–XI show that, when technical and correction problems are met, critical scattering may be observed in the small- and intermediate-x range by neutron scattering with an accuracy comparable to that of light scattering. Since the critical regime is more easily reached with neutrons, the large-x range may then be determined with a better precision; in particular, the critical index η has been determined with a precision not yet obtained. This favorable conclusion is probably largely due to the high sensitivity of neutrons to fluctuations of concentration in the Na-ND_3 system.

From these results, several points concerning scaling and the several approximations of the scattering function may be raised.

A conclusive indication of the validity of scaling hypothesis is to find the same value of the index η from Eq. (10) and from the shape of the scattering function at large x; following Tracy and McCoy,[3] if Eq. (10) is rewritten as $\tilde{\eta}=2-\gamma/\nu$, scaling will be true if η defined by Eq. (12) is such that $\tilde{\eta}=\eta$. The value of $\tilde{\eta}$ has been determined in Sec. X (0.0283 ± 0.002) and different evaluations of η have been found in Sec. XI; only calculations carried out at a single temperature or using method a (FB and FL) give really access to η; results obtained with method b which makes use of Eq. (10) give a mixture of $\tilde{\eta}$ and η. It is noted that all results obtained with method b are very close to those found from Eq. (10) using the observed values of γ and ν. Three average values of "pure" η were found: single run, $\langle\eta\rangle=0.031$, error 0.005, FB with $C_1=0.91$; regrouped data FB(a), $\langle\eta\rangle=0.029$, error 0.0011; regrouped data FL(a), $\langle\eta\rangle=0.0305$, error 0.0015.

From these results, the difference between η and $\tilde{\eta}$ should not exceed 0.002. Considering the errors, the factor G_f, which is as good with method b as with method a, and the results obtained from simulated experiments, one must conclude that detection of such a small difference from the present set of data (with their statistical uncertainties) is at the limit of significance.

Another remark concerns the parameter C_1 which was nicely obtained from FB(b) very near theoretical predictions and the evaluation obtained from the Fisher equation (0.91 ± 0.002). Using the LX(a) or FL(a) equation, the constant C_1 was systematically found near 0.93 with a somewhat larger error (0.01). This could be due to a bad evaluation of C_2 and C_3, but this irreducible difference is not well understood. From the experimental point of view, there is some ambiguity in the FL equation, being the more precise equation but with many parameters.

All calculations were strongly supported by simulated experiments, with random Gaussian errors, which were treated exactly in the same way as in real experiments. Many questions were then answered; for example (Sec. IX), it was found that precise values of correlation lengths could be obtained from the COZ equation in the 0–20 x range even if the values of the coefficients ($\alpha=0.11$, $\nu=0.628$, $\eta=0.03$) were actually slightly different from those used in the evaluation of Bray.[4] It was thus also shown that the precision obtained on the index η [±0.005 from a single run and ±0.001 from regrouped data (method b)] was almost exactly that expected from the experimental statistical error made on the counting rate.

That gives confidence that statistical errors are well handled. A constant concern during the whole data process was to track possibilities of systematic errors which

may be very difficult to detect; the more fragile point is certainly the background evaluation (part VI). Several backgrounds have been checked even at the limit of likeness. The results are typically the following. (i) For single run fits, as reported in Figs. 9 and 10, values of η may be shifted by 0.015 from presented results and a marked temperature effect is detected (for example $\eta=0.045$ near T_c and 0.023 at 1 deg from T_c); the factor G_f decreases in the 0.01–0.20 range and the average uncertainty remains near 0.005. (ii) Values of η remain in the 0.03 range for regrouped data but G_f was then, in most cases, very poor (below 0.001) and the precision on η was near 0.005 as for single run fits. This indicates that all data did not fall correctly on the same $g(x)$ curve when regrouping. The increase of precision from 0.005 to 0.0015 when data are regrouped is certainly a good indication that systematic errors have been minimized.

No mention was made on corrections to scaling. Attempts to include such a correction[21,22] were not very successful; the additional parameters are indeed too closely correlated to the leading terms and convergence is not even always obtained. To avoid the problem, as indicated in Sec. IX, all calculations aimed to determine the critical indices ν, γ, and η, and the shape of the scattering function have been made using data collected very near the critical point (0.5 K or $t<2\times10^{-3}$). Many fits were performed, in addition to that reported in Table II, to check all the results with different temperatures (runs chosen for data regrouping) and with x range. All parameters presented in Table II were found remarkably constant throughout these different treatments, except for an increase of the uncertainty observed when the number of data points decreases too much. This behavior could be expected by inspecting the values of G_f tests; for example a value of G_f of 0.54 (fit 11 of Table II) obtained with 350 points with three fitted parameters indicates that the data form a very coherent set, which is well accounted for by the equation. In this case only three points had a ratio of residual/standard error larger than 2.5. Such a large value of G_f shows at the same time the limit of what can be extracted from the data set and its intrinsic statistical error.

ACKNOWLEDGMENTS

The Laboratoire de Chemie Physique is associated with the Centre National de la Recherche Scientifique (Unite Associée No. 253).

[1]M. E. Fisher and A. Aharony, Phys. Rev. B **10**, 2818 (1974).
[2]H. B. Tarko and M. E. Fisher, Phys. Rev. B **11**, 1217 (1975).
[3]C. A. Tracy and B. M. McCoy, Phys. Rev. B **12**, 368 (1975).
[4]A. J. Bray, Phys. Rev. B **14**, 1248 (1976).
[5]J. V. Sengers, in *Phase Transitions,* edited by M. Levy, J. C. Le Guillou, and J. Zinn-Justin (Plenum, New York, 1982).
[6]M. E. Fisher, J. Math. Phys. **39**, 944 (1964).
[7]M. A. Moore, D. Jasnow, and M. Wortis, Phys. Rev. Lett. **22**, 940 (1969).
[8]J. C. Le Guillou and Z. Zinn-Justin, Phys. Rev. Lett. **39**, 95 (1977); Phys. Rev. B **21**, 3976 (1980).
[9]D. Schwahn and D. Woermann, Ber. Bunsenges. Phys. Chem. **90**, 339 (1986).
[10]R. Schneider, L. Belkoura, J. Schelten, D. Woermann, and B. Chu, Phys. Rev. B **22**, 5507 (1980).
[11]P. Damay, F. Leclercq, and P. Chieux, Physica B **156**, 223 (1989).
[12]M. Katsumoto and P. Damay, J. Phys. Chem. **79**, 2928 (1975).
[13]A. B. Bhatia and D. E. Thornton, Phys. Rev. B **2**, 3004 (1970).
[14]K. Kawasaki, Phys. Rev. A **6**, 1750 (1970).
[15]A. N. Garroway and R. M. Cotts, Phys. Rev. A **7**, 635 (1973).
[16]R. E. Ghosh, ILL Report No. 81-GH29T (1981).
[17]P. Damay, F. Leclercq, and P. Chieux, J. Phys. Chem. **88**, 3734 (1984).
[18]C. A. Kraus, E. S. Carney, and W. C. Johnson, J. Am. Chem. Soc. **49**, 2206 (1927).
[19]W. H. Press, B. P. Flannery, S. A. Teukolsky, and W. T. Vetterling, *Numerical Recipes,* (Cambridge University Press, New York, 1987).
[20]F. Leclercq, P. Damay, and P. Chieux Z. Phys. Chem. Neue Folge **1**, 183 (1987).
[21]F. J. Wegner, J. Phys. A **8**, 710 (1975).
[22]P. W. Schmidt and M. Chandrasekhar, Phys. Rev. B **24**, 2773 (1981).